

MEASUREMENT OF THE EXTRACTION KICKER SYSTEM IN J-PARC RCS

J. Kamiya[#], M. Kuramochi, M. Kinsho, T. Ueno, T. Takayanagi, O. Takeda, M. Watanabe, M. Yoshimoto, JAEA/J-PARC, Tokai, Naka, Ibaraki, Japan

Abstract

Kicker magnet system in the J-PARC RCS is now under construction at JAEA (Japan Atomic Energy Agency). Their role in RCS is to kick the accelerated 3 GeV proton beam to the following extraction line at a repetition rate of 25 Hz. They are installed in the vacuum chambers to prevent discharge. We performed the voltage apply test in vacuum up to the operation voltage. We also investigated the time dependence of the magnetic field at the operation voltage and repetition rate. The severe specification of 2 % is required on the magnetic field to achieve the large beam power of 1 MW. Therefore we carefully performed the magnetic field mapping by using 3-axes stage with a short search coil. The distribution of the magnetic field (B_y) was systematically measured for the three types of kickers. Integrated magnetic field (BL) was calculated by the B_y values and their distribution is shown.

OUTLINE OF KICKER SYSTEM

Kicker magnet system in the J-PARC RCS is now under construction at JAEA (Japan Atomic Energy Agency). Their role in RCS is to kick the accelerated 3 GeV proton beam to the following extraction line at a repetition rate of 25 Hz. Details of the kicker system is reported in Ref [1]. Therefore we briefly show the outline of our kicker system here. Eight kicker magnets are installed in the extraction section of the RCS. Three types of kicker magnets (type-L, M, S), distinguished by the difference in the size of their apertures are placed in order of L, M, S, (Q), S, S, M, L, L, where Q is a vertically defocused quadrupole magnet. They are installed in vacuum chambers because high voltage of 30 kV, which corresponds to charging voltage of 60kV due to pulse forming network (PFN), is applied. Fig. 1 shows a design drawing of a type-L kicker magnet [2]. Our kicker magnets are transmission line type [3]. The gap height is 199 mm for type-L. For type-M and S, they are 173 mm 153 mm, respectively. Ferrite is used as a magnetic core because of its good high-frequency properties. Aluminum alloy is used for the high voltage plates and earth plates. These parts form a distributed-parameter line. The characteristic impedance is designed to be 10 ohm.

MAGNETIC FIELD MEASUREMENT

There are mainly two measurement settings, which are measurement in vacuum and in air. In order to apply the operation charging voltage of 60 kV, the kicker has to be installed in vacuum to prevent discharge. However, the measurement of the magnetic field distribution is very

difficult in vacuum. Therefore distribution measurement was performed in the air at the charging voltage of 20 kV.

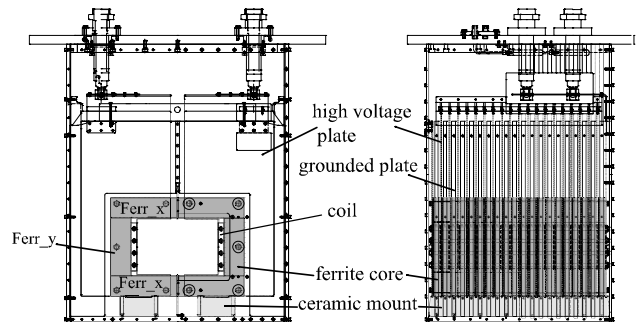


Figure 1: Design drawing of the kicker system.

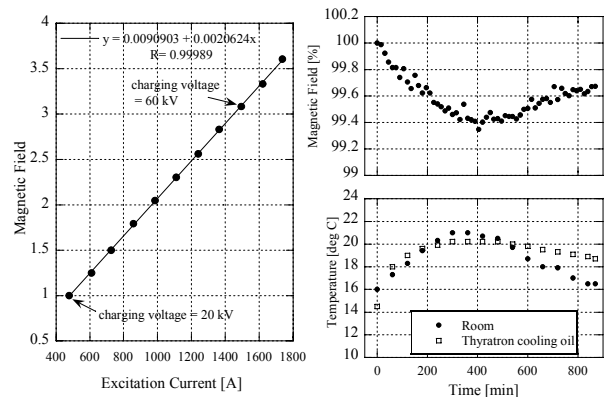


Figure 2: Results of the exciting test in vacuum. Left panel shows the B-I curb. Right two panels show the magnetic field and the temperature of the room and thyatron cooling oil during 14 hours continuous excitation test.

Exciting Test in Vacuum

Exciting test to apply the operation voltage was performed in a test chamber. The size of the chamber is designed to install one magnet. The vacuum pump was a turbo molecular pump with its exhaust velocity of 1000 l/s. Pressure is about $10^{-4} \sim 10^{-3}$ Pa when a magnet was installed. A search coil of 6 turns with 20 mm diameter is used to measure the induced current by magnetic field. Output signal from the search coil was taken from an insulated BNC connector at a vacuum flange and integrated by a resistance-capacitance circuit. We carefully choose the resistance and capacitance whose dependence on temperature is small. Fig. 2 shows the

[#]kamiya.junichiro@jaea.go.jp

results of the excitation test in vacuum. Left panel shows the relation between exciting current and magnetic field, B-I curb. Magnetic field represents the average of the flat top which was measured by the search coil at the center of the aperture. They are normalized by the value at charging voltage of 20 kV. Current was measured by a current transformer PEARSON MODEL 110 which was installed at a load cable. The charging voltage was increased every 5 kV from 20 kV to 75 kV. R in the graph represents the correlation coefficient for the least-square method of the linear line. Linearity of the magnetic field to the current was maintained in this region.

We also measured time stability of magnetic field. Right two panels in Fig. 2 shows the result of the exciting test at 60 kV 25 Hz for 14 hours. Temperature was also measured during the test. It is noticed that value of the flat top depends on the temperature. Percentage of change is about 0.1 %/deg C. Because the change the magnetic field is relatively slow, we can control the charging voltage to suppress this fluctuation by monitoring the load current in the actual operation.

Magnetic Field Distribution

Fig. 3 shows the setup of the magnetic field mapping. Measurement was carried out in the clean room of class 10000. The 3-axes support was used in the measurement. Definition of the direction of the 3 axes is also shown in Fig. 3. Origin of the 3 axes is defined by the center of the aperture. The probe was the same search coil which was used in the measurement in vacuum. Each axis of the stage was precisely aligned. The maximum disagreement from right angle was less than 2 mrad, which was an acceptable misalignment to perform the field mapping. Magnetic field measurement was performed with the charging voltage of 20 kV. The following results of the field mapping are expected to be maintained at operation voltage of 60 kV because the linearity of B-I curb as shown in Fig. 2.



Figure 3: Setup of the magnetic field mapping. Definition of the direction of the 3 axes is also shown.

Fig. 4 shows the distribution of the magnetic field B_y along the z direction for the type-L magnet with serial No.7. Upper panel represents the comparison at different x in the medium plane ($y = 0$). Lower panel represents the

comparison at different y for the same x ($=0$). The step of the z direction was 40 mm. As shown in the both panels, leak field disappears at about 300 mm from the core edge because of the wide aperture. At the side end, $x = +120$ mm, the values of B_y near the center, $z = 0$, are larger than those at $x = 0$ because of the leakage field from the ferrite core, shown by Ferr_y in Fig. 1. It is noticed from the lower panel in Fig. 4 that the magnetic field flux is concentrated near the core edge.

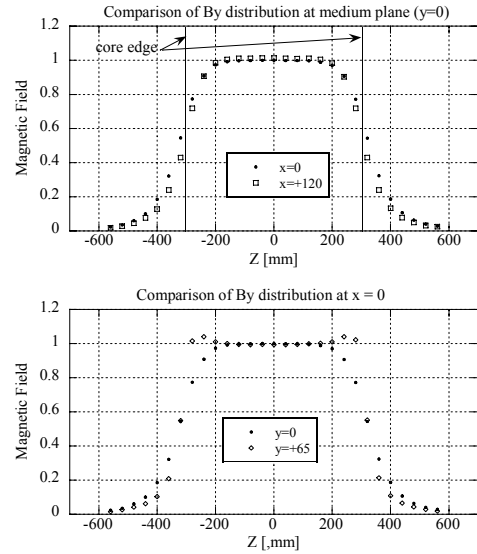


Figure 4: B_y distribution along the z axis. Each value is normalized by the values at the origin.

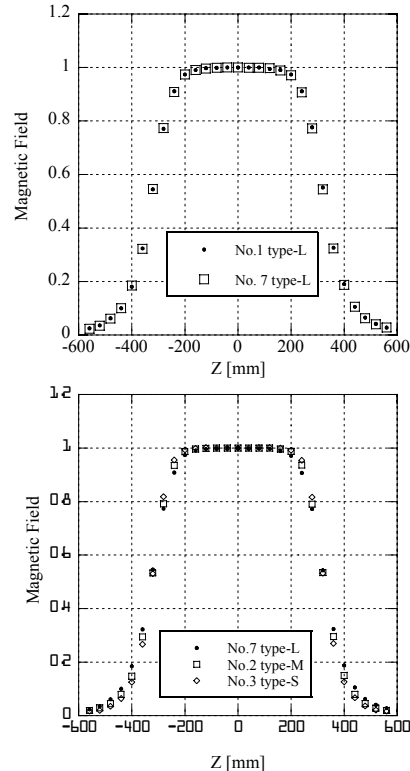


Figure 5: Comparison of B_y distribution. Upper and lower panels show between magnets of the same type and comparison between different types of magnets, respectively.

Fig. 5 shows the comparison of B_y distribution between magnets. Upper panel shows the comparison between the same type of magnets. Each value is normalized by the value at the origin of serial No.1. B_y distributions agree with each other well. Lower panel in Fig. 5 shows the comparison between different types of magnets. There were more leakage field in the case of the larger vertical aperture.

Integrated magnetic field BL was calculated by using the B_y values measured along the z axis as

$$BL = \sum B_y \Delta z \tag{1}$$

,where Δz represents the measurement step shown in Fig. 4 and 5. Fig. 6 shows the BL distribution of the type-L magnet with serial No. 7. Closed circles are BL in the medium plane. Closed squares and rhombuses represent BL in the upper and lower edge of the aperture, respectively. They have error bars of 0.3 %, which was calculated from the change rate of value at origin during the measurement. Good field region of 2 % is required for the 324pi mm-mrad beam, which is assumed for 3 GeV beam. The horizontal beam size corresponds to about $\Delta x = 160\text{mm}$, which is within the good field region of 2 %. BL distribution in upper and lower edge of the aperture is larger than 2 %. Effect of the magnetic field out of requested value on beam loss will be investigated. The allocation of ferrite cores is symmetric with respect to the x-axis. However, high voltage plates and grounded plates are not symmetric. Therefore, the BL distribution in the symmetry plane is not the same as each other.

Fig. 7 shows the comparison of the BL distribution at medium plane between different types of magnets, L, M, and S. As described before, they are distinguished by the difference in the size of their apertures. The distribution of the BL is the same within error bars between different types of magnets.

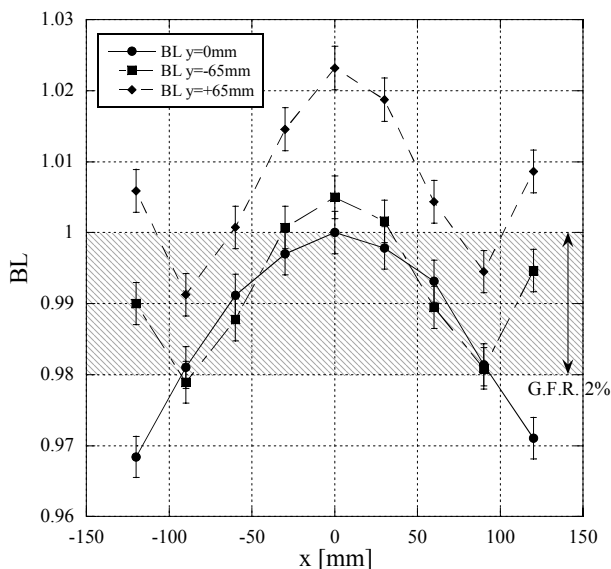


Figure 6: BL distribution along the horizontal axis for three typical planes. Data is normalized by the BL values at $x = 0, y = 0$.

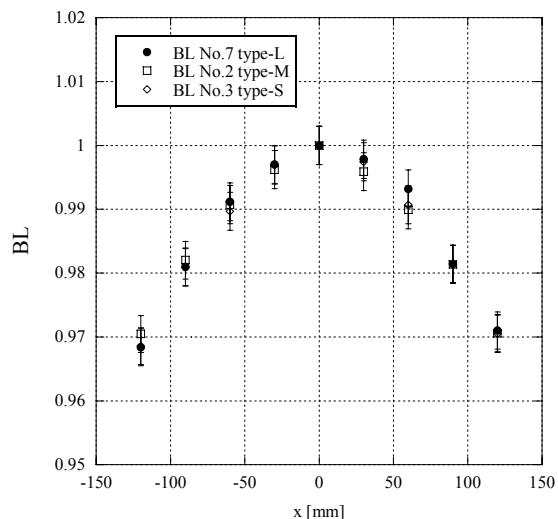


Figure 7: Comparison of the BL distribution in the medium plane between three types of magnets, L, M, and S. Data is normalized by the BL values at $x = 0$ of each magnet.

CONCLUSION

We measured the magnetic field of the RCS extraction kicker magnet. Excitation voltage was applied in vacuum up to the operation value of 60 kV. The time stability was also investigated by excitation test for 15 hours. Magnetic field mapping was performed for the different types of the magnets.

REFERENCES

- [1] J. Kamiya, T. Takayanagi, T. Kawakubo, S. murasugi, E. Nakamura, "Kicker Magnet System of the RCS in J-PARC," the proceedings of the 19th International Conference on Magnet Technology (MT-19), IEEE Transaction of Applied Superconductivity, in press.
- [2] NEC/TOKIN Corporation, <http://www.nec-tokin.com/>
- [3] G. Nassibian, "TAVELLING WAVE KICKER MAGNETS WITH SHARP RISE AND LESS OVERSHOOT", IEEE Transactions on Nuclear Science, Vol. NS-26, No. 3, June 1979.